Response of Small Heat Shock Proteins in Diabetic Rat Retina

Vadde Sudhakar Reddy, Ganugula Raghu, Singareddy Sreenivasa Reddy, Anil Kumar Pasupulati, Palla Suryanarayana, and Geereddy Bhanuprakash Reddy

Biochemistry Division, National Institute of Nutrition, Hyderabad, India

Correspondence: Geereddy Bhanuprakash Reddy, National Institute of Nutrition, Tarnaka, Jamai-Osmania, Hyderabad - 500 007, India; geereddy@yahoo.com.

Submitted: July 1, 2013
Accepted: October 16, 2013

Citation: Reddy VS, Raghu G, Reddy SS, Pasupulati AK, Suryanarayana P, Reddy GB. Response of small heat shock proteins in diabetic rat retina. *Invest Ophthalmol Vis Sci*. 2013;54:7674–7682. DOI:10.1167/iovs.13-12715

Purpose. Small heat shock proteins (sHsps) have a critical role under stress conditions to maintain cellular homeostasis by their involvement in protein-folding and cytoprotection. The hyperglycemia in diabetes may impose cellular stress on the retina. Therefore, we investigated the expression of sHsps, phosphoregulation of αB-crystallin (αBC), and their localization in the diabetic rat retina.

Methods. Diabetes was induced in rats and maintained on hyperglycemia for a period of 12 weeks. The expression of sHsps, HSFs, and phosphorylated sHsps was analyzed by quantitative (q) RT-PCR and immunoblotting. The solubility of sHsps was analyzed by detergent solubility assay. Cellular localization of sHsps and phosphorylated αBCs was examined by immunohistochemistry.

Results. Of 10 sHsps, five sHsps were detected in the rat retina. Among those, increased expression for αA-crystallin (αAC), αBC, and Hsp22, and decreased expression for Hsp20 were seen in the diabetic retina, whereas Hsp27 mRNA levels were increased, while protein levels were decreased. While the expression of HSFs was either unaltered or decreased, expression of hypoxia inducible factor-1α (HIF-1α) was increased in the diabetic retina. The phosphorylation of αBC at Ser45 and Ser19 was increased in the retina of diabetic rats. However, phosphorylation of αBC at Ser59 was decreased in the soluble fraction with a concomitant increase in the insoluble fraction. Moreover, diabetes activated the p38MAPK signaling cascade by increasing the p-p38 MAPK in the retina. Further, diabetes induced the aggregation of Hsp27, αAC, αBC, and pS59-αBC in the retina. A strong immunoreactivity of Hsp27, αAC, αBC, and phosphorylated αBC was localized in different retinal layers of diabetic rats.

Conclusions. The results indicate an upregulation of αAC, αBC, and Hsp22, but their solubility was compromised in the diabetic retina. There was increased phosphorylation at Ser59, Ser45, and Ser19 of αBC under diabetic conditions. Localization of sHsps and their phosphorylated forms was dispersed to many layers of the retina in diabetes. These results suggest that sHsps may be protecting the retinal neurons in chronic diabetes.

Keywords: diabetic retinopathy, sHsp, HSF, streptozotocin, phosphorylation, type 1 diabetes

Diabetes and its complications are a major cause of morbidity and mortality all over the world. Diabetic retinopathy (DR) is one of the most common microvascular complications of diabetes and ranks as a common cause of blindness worldwide.[1] Diabetic retinopathy could become a major threat to public health in the future due to the global prevalence of diabetes, which is projected to affect 552 million people by 2030.[2] Diabetic retinopathy occurs in 70% of all people with diabetes for more than 15 years. The etiology and pathogenic mechanisms underlying DR still are largely unknown, albeit numerous studies implicate oxidative stress, advanced glycation end products, inflammation, neurodegeneration, and so forth. The conditions created during diabetes are known to increase oxidative stress as well as downregulate the cellular antioxidant defense systems.[3,4] Uncontrolled oxidative stress represents a characteristic feature of diabetes and diabetic complications, such as DR.[5] It has been shown that expression of stress proteins is elevated in several pathophysiologic conditions to offer protection against tissue damage.

Heat shock proteins (Hsps), also called stress proteins, are elevated in a variety of stress conditions, including high temperature (heat shock), hypoxia, ischemia, endotoxins, heavy metals, and reactive oxygen species. A group of low-molecular weight Hsps, ranging in monomer size from 16 to 27 kDa, are referred to as small Hsps (sHsps). The sHsps are heterogeneous and are characterized by a conserved C-terminal region, called the α-crystallin domain. A subfamily of 10 sHsps exists in mammals[6] that include Hsp27/ Hsp25 of rodents (HSPB1), myotonic dystrophy protein kinase (MKBP, HSPB2), HSPB3, αA-crystallin (αAC, HSPB4), αB-crystallin (αBC, HSPB5), Hsp20 (HSPB6), cvHsp (HSPB7), Hsp22/H11/H2IG1 (HSPB8), HSPB9, and sperm outer dense fiber protein (ODF, HSPB10). The sHsps function characteristically as molecular chaperones assisting in assembly, stabilization, internal transport of intracellular proteins, maintenance of the cytoskeleton architecture, and protection against programmed cell death.[7,8] The

phenomenon of induction of Hsps is believed to be regulated by a family of heat shock transcription factors (HSFs). There are three known HSFs in mammals: HSF1, HSF2, and HSF4. Among these, HSF1 is considered to be the universal HSF and it responds to an external stress signal, such as high temperature. The HSF2 is associated with developmental control whereas HSF4 regulates postnatal expression of Hsps.[9] Hypoxia inducible factor-1α (HIF-1α), another transcription factor that is activated specifically by decreased tissue oxygen supply, regulates rapid induction of Hsp synthesis.[10,11] The chaperone activity and cytoprotective functions of sHsps are regulated by phosphorylation.[12,13] The αBC is a major sHsp tightly regulated by phosphorylation at three sites; serines at positions 59 (S59), 45 (S45), and 19 (S19). While the S59 of αBC is phosphorylated by p38–mitogen-activated protein kinase (p38MAPK), S45 is phosphorylated by extracellular signal-regulated kinase (ERK).[14,15] The kinase responsible for phosphorylation of S19 of αBC is unknown.

Several studies have reported an increased expression of αAC and αBC in various tissues, including the retina in rodent models of type 1 diabetes, and implicated their role in preventing retinal cell death.[16–18] However, the expression of remaining members of sHsps, the role of HSFs, and, more so, phosphoregulation of sHsps still is unknown in the diabetic retina. To our knowledge, there are no reports demonstrating the status of phosphorylation and phospho-specific localization of sHsps in the diabetic rat retina. Therefore, we examined comprehensively the expression of all sHsps, HSFs, their solubility and regulation of the major sHsp, αBC, by kinase-mediated phosphorylation in the diabetic rat retina.

Materials and Methods

Materials

Streptozotocin (STZ), Tri-reagent, Triton X-100 (Triton-X), acrylamide, bis-acrylamide, ammonium persulfate, β-mercaptoethanol, SDS, TEMED, PMSF, aprotinin, leupeptin, pepstatin, anti-actin antibody (Cat. No. A5060), horseradish peroxidase (HRP)–conjugated anti-rabbit (A6154), and anti-mouse (A9044) secondary antibodies were purchased from Sigma Chemicals (St. Louis, MO). Bradford reagent was obtained from Bio-Rad Laboratories, Inc. (Hercules, CA). Nitrocellulose membrane was obtained from Pall Corporation (Pensacola, FL). Anti-Hsp27 (MA3-014), anti-Hsp20 (PA1-29447), anti-HSF1 (PA3-017), anti-HIF1α (PA1-16601), and specific antibodies recognizing three phosphorylated residues (S19, S45, and S59) of αBC were obtained from Thermo Scientific-Pierce (Rockford, IL). Anti-MKBP (18-821-485217) and anti-Hsp22 (18-821-485201) were obtained from Genway (San Diego, CA). Anti-αAC and anti-αBC antibodies were produced in the rabbit as reported previously.[19] Anti-p38MAPK (#9212S) and anti–p-p38MAPK (#9211S) antibodies were purchased from Cell Signaling Technology, Inc. (Beverly, MA). Anti-HSF2 (sc-13056), anti-HSF4 (sc-19864), glyceraldehyde-3-phosphate dehydrogenase (GAPDH, sc-25778), and HRP-conjugated anti-goat (sc-2020) secondary antibodies were purchased from Santa Cruz Biotechnology, Inc. (Dallas, TX). The RNA purification kit was obtained from Qiagen, Inc. (Valencia, CA). The high capacity cDNA reverse transcription kit (4368814) and Power SYBR Green Master Mix (4374966) were obtained from Applied Biosystems (Warrington, UK). All primers were procured from Integrated DNA Technologies (Coralville, IA). An enhanced chemiluminescence (ECL) detection kit was obtained from GE Health Care (Buckinghamshire, UK). Vectashield mounting medium containing 4′6-diamidino-2-phenylindole (DAPI) was obtained from Vector Laboratories (Burlingame, CA). Alexa Fluor 488–conjugated anti-rabbit and Alexa Fluor 555–conjugated anti-mouse antibodies were obtained from Molecular Probes (Eugene, OR).

Animal Care and Experimental Conditions

Three-month-old male Wistar-NIN rats with average body weight of 230 ± 14 g were obtained from National Center for Laboratory Animal Sciences, National Institute of Nutrition, Hyderabad, India, and maintained at a temperature of 22 ± 2°C, 50% humidity, and 12-hour light/dark cycle. The control rats ($n = 10$) received 0.1 M sodium citrate buffer, pH 4.5, as a vehicle, whereas the experimental rats received a single intraperitoneal injection of STZ (35 mg/kg) in the same buffer. At 72 hours after STZ injection, fasting blood glucose levels were monitored and animals with blood glucose levels > 150 mg/dL were considered for the experiment ($n = 10$). Control and diabetic animals were fed with AIN-93 diet ad libitum. Body weight and blood glucose concentration of each animal were measured weekly. At the end of 12 weeks, rats were fasted overnight and sacrificed by CO_2 asphyxiation. Eyeballs were dissected out immediately, and cut into two hemispheres to remove the lens and vitreous body. Care was taken to collect the retina intact from the concave region of the eyeball adjacent to the optical nerve. Institutional and national guidelines for the care and use of animals were followed, and all experimental procedures involving animals were approved by the Institutional Animal Ethical Committee (IAEC) of the National Institute of Nutrition. We adhered to the ARVO Statement for the Use of Animals in Ophthalmic and Vision Research. The 12-week diabetes duration was chosen because it leads to retinopathy-like complications, including impaired insulin receptor signaling, increased neuronal cell death, astrocyte defects, microvascular leakage, and microglial cell activation in rat models of type 1 diabetes.[20–24]

Biochemical Estimations

Glucose and glycosylated hemoglobin (HbA1c) in blood were measured by the glucose oxidase–peroxidase (GOD–POD) method and ion-exchange resin, respectively, using commercially available kits (Biosystems, Barcelona, Spain).

Quantitative Real-Time PCR (qRT-PCR)

Total RNA was extracted from control and diabetic rat retina using Tri-reagent according to the manufacturer's instructions. Isolated RNA was purified further by the RNeasy Mini Kit, and quantified by measuring the absorbance at 260 and 280 nm on an ND1000 Spectrophotometer (NanoDrop Technologies, Wilmington, DE). Two to 4 μg total RNA were reverse transcribed using a high capacity cDNA reverse transcription kit. Reverse transcription reaction was done using a thermocycler (ABI-9700) and reaction conditions were as follows: initial RT for 10 minutes at 25°C, followed by 37°C for 120 minutes, and inactivation of reverse transcriptase at 84°C for 5 minutes. Real-time PCR (ABI-7500) was performed in triplicates with 25 ng cDNA templates using SYBR green master mix with gene-specific primers (see Table). Normalization and validation of data were carried out using β-actin as an internal control, and data were compared between control and diabetic samples according to the comparative threshold cycle ($2^{-\Delta\Delta ct}$) method. The reaction conditions were as follows: 40 cycles of initial denaturation temperature at 95°C for 30 seconds, followed by annealing at 52°C for 40 seconds, and extension at 72°C for 1 minute, and product specificity was analyzed by melt curve analysis.

Table. List of Primers and Their Sequence Used in the Study

Gene	Sequence
β-Actin	5′ GAG AAG AGC TAT GAG CTG CC 3′
	5′ CTC AGG AGG AGC AAT GAT CT 3′
Hsp27	5′ GAT GAA CAT GGC TAC ATC TCT C 3′
	5′ CTG ATT GTG TGA CTG CTT TG 3′
MKBP	5′ ACT GTG GAC AAC CTG CTA GA 3′
	5′ GGA GAT GTA GAC CTC ATT GAC T 3′
HSPB3	5′ TCT TGC AGA GGA CTC AGA CT 3′
	5′ GTT TGT ACT GTC TGG TGA AAC TC 3′
αAC	5′ GAA AGA AGA TAT TTA TGC AGT GG 3′
	5′ CCT CAA AGA TAT TGG ATA TGG TA 3′
αBC	5′ TGG AGT CTG ACC TCT TTT CTA C 3′
	5′ AGA ACC TTG ACT TTG AGT TCC 3′
Hsp20	5′ AGA GGA AAT CTC TGT CAA GGT 3′
	5′ GGA TAG ACA GAA CAC CCT 3′
cvHsp	5′ AGT TTA CTG TGG ACA TGA GAG AC 3′
	5′ CTG GAC ATG TTC TGT GTG TG 3′
Hsp22	5′ AGA ACT GAT GGT AAA GAC CAA G 3′
	5′ AGAAAG TGA GGC AAA TAC AGTC 3′
HSPB9	5′ GAA CCA AGT TTC CAG ATG AA 3′
	5′ GAG AGG TAG GCA CTT ATT TTG TC 3′
ODF	5′ GGA CAG AGA ACT AAG ACA ATT GAG 3′
	5′ CAG TAC AGC TTG TAG TCA CAC AG 3′
HSF1	5′ CCA GCA GCA AAA AGT TGT CA 3′
	5′ TGG TGA ACA CAG CAT CAG AGG AG 3′
HSF2	5′ TGA TCC CTC CAG CCA GTA TC 3′
	5′ CAG GTT GGA GGA GCC ATT TA 3′
HSF4	5′ GTG GCC TGC TAA GAC CAG AC 3′
	5′ CGG TTG GCC TTA GGG TTC AGG GGG G 3′
HIF-1α	5′ GAA ACC GCC TATGAC GTG CT 3′
	5′ ATC GAG GCT GTG TCG ACT GA 3′

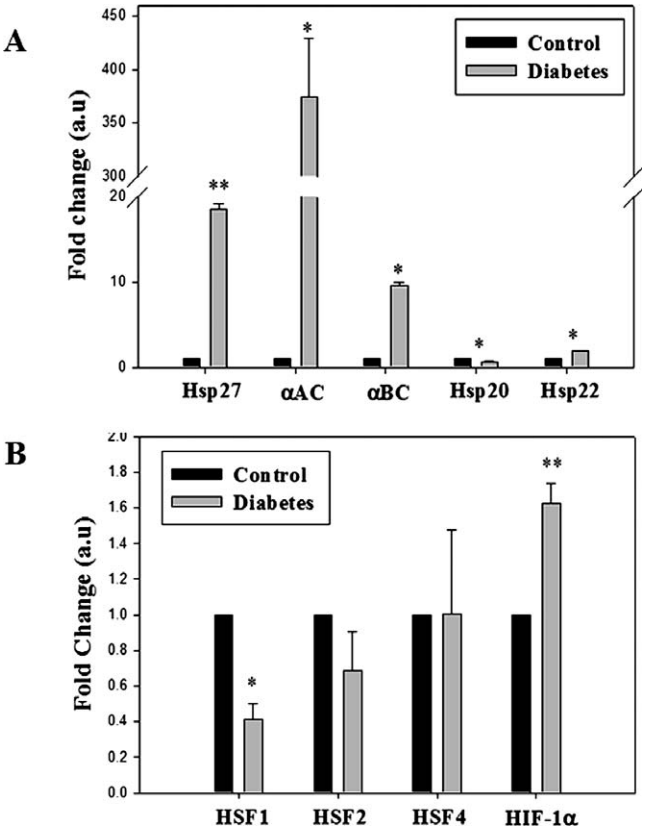

Figure 1. Quantitative RT-PCR analysis of sHsps (**A**) and HSFs (**B**) in retinas of control and diabetic rats. Effect of STZ-induced diabetes on the expression of sHsp family and HSFs in retinas was analyzed by qRT-PCR. Relative expression pattern was analyzed by the comparative threshold cycle ($2^{-\Delta\Delta ct}$) method. Expression values were represented as fold change over control on an arbitrary scale after normalization with actin. Data represent mean ± SEM of three independent experiments.*$P < 0.05$, **$P < 0.01$ compared to the control.

Whole Tissue Lysate Preparation

Retina was homogenized in a buffer containing 20 mM Tris, 100 mM NaCl, 1 mM EDTA, 1 mM DTT (TNE buffer, pH 7.5), and protease inhibitors. Homogenization of the retina was performed on ice using a glass homogenizer and the homogenate was centrifuged at 12,000*g* at 4°C for 20 minutes. The protein concentrations were measured by Bradford reagent.

SDS-PAGE and Immunoblotting

Equal amounts of protein (30 μg for αAC and αBC; 50 μg for Hsp27, phosphorylated αBCs, p38MAPK, p-p38MAPK, HSF1, and HIF-1α; 80 μg for Hsp20, Hsp22, HSF2, and HSF4) were subjected to 12% SDS-PAGE and transferred to nitrocellulose membranes (0.22 μm pore size) by Western blot transfer system (Bio-Rad Laboratories, Inc.) at a voltage of 40 V for 3 hours. Nonspecific binding was blocked with 5% nonfat dry milk powder in PBST, and incubated overnight at 4°C with monoclonal anti-Hsp27 (mouse, 1:500), polyclonal anti-αAC, anti-αBC (rabbit, 1:3000), polyclonal anti-pS59, pS45, pS19-αBC (rabbit, 1:2000), polyclonal anti-Hsp20 (rabbit, 1:10,000), polyclonal anti-Hsp22 (rabbit, 1:1000), polyclonal anti-p38MAPK (rabbit, 1:1000), polyclonal anti-p-p38MAPK (rabbit, 1:1000), polyclonal anti-HSF1 (rabbit, 1:10,000), polyclonal anti-HSF2 (rabbit, 1:500), polyclonal anti-HSF4 (goat, 1:500), polyclonal anti–HIF-1α (rabbit, 1:2000), polyclonal anti-actin (rabbit, 1:500), and polyclonal anti-GAPDH (rabbit, 1:500) antibodies diluted in PBS-Tween (PBST). After washing with PBST, membranes then were incubated with anti-rabbit IgG (1:3500) or anti-mouse IgG (1:3500), or anti-goat IgG (1:10,000) secondary antibodies conjugated to HRP. The immunoblots were developed using an ECL detection kit and digital images were recorded by Image analyzer (G:Box iChemi XR, Syngene, UK). Quantification of band intensity was performed with ImageJ software (available in the public domain at http://rsbweb.nih.gov/ij/).

Detergent Soluble Assay

For analyzing detergent solubility, retina was homogenized in TNE buffer containing 0.5% Triton-X. Following centrifugation, homogenate was separated as supernatant containing detergent soluble fraction and the pellet containing insoluble protein fraction, and this pellet was washed with PBS, rehomogenized, sonicated, and dissolved in Lammelli buffer. The samples then were analyzed by immunoblotting as described above.

Immunohistochemistry

The dissected eyeball was placed immediately in 4% paraformaldehyde in phosphate buffer (pH 7.2), fixed overnight, embedded in paraffin blocks, and cut into 4 μm sections. The sections were deparaffinized by incubating in xylene for 5 minutes followed by dehydration in decreasing grades of ethanol (100%, 95%, and 70%). Deparaffinized sections were boiled in 0.01 M Na-citrate, pH 6.0, for 10 minutes at 60°C and blocked with blocking solution (3% horse serum, 3% BSA, 0.3%

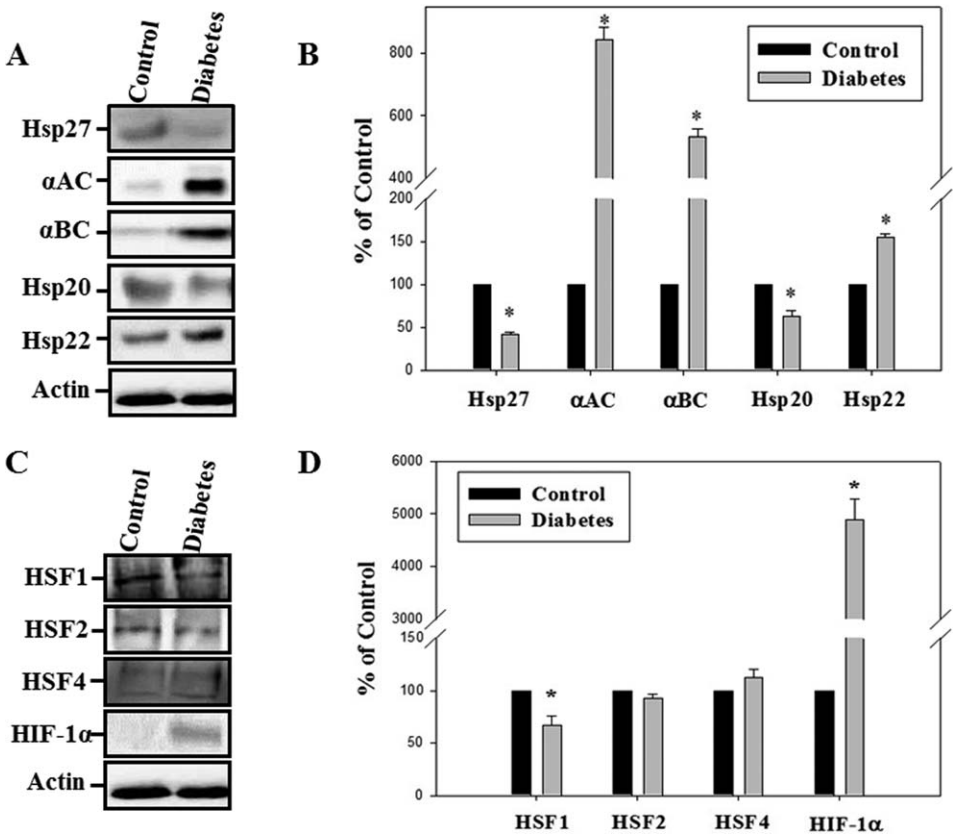

FIGURE 2. Immunoblot analysis of sHsps (**A**) and HSFs (**C**) in retinas of control and diabetic rats. Amounts of 30 μg protein were loaded on SDS-PAGE for αAC and αBC; 50 μg for Hsp27, HSF1, and HIF-1α; and 80 μg for Hsp20, Hsp22, HSF2, and HSF4. Quantification of sHsp (**B**) and HSF (**D**) immunoblots in retinas of control and diabetic rats; expression was normalized for actin expression and results are represented as percent of control. Data represent mean ± SEM of three independent experiments. $^*P < 0.05$ compared to the control.

Triton-X in Tris-buffered saline [TBS]). Slides were washed 3 times with TBS, and incubated in TBS with anti- Hsp27 (1:200), anti-αAC (1:50), anti-αBC, anti-pS59, pS45, and pS19-αBC (rabbit, 1:100) antibodies overnight at 4°C. Slides were washed 3 times with TBS and the binding of primary antibodies was visualized by Alexa Fluor 488–conjugated anti-rabbit (1:1000) and Alexa Fluor 555–conjugated anti-mouse (1:1000) IgG antibody for 1 hour. Sections were mounted in medium containing DAPI and visualized using a Leica laser microscope (LMD6000; Leica Microsystems Vertrieb GmbH, Wetzlar, Germany).

Statistical Analysis

Student's *t*-test was used for the comparison between two groups. Values of $P < 0.05$ were considered significant. All data are presented as mean ± SE and expressed as a fold change over control.

RESULTS

Blood Glucose, HbA1c Levels, and Body Weights. The mean blood glucose levels of control rats were 91.5 ± 6.17 mg/dL and increased significantly to 390.1 ± 48.7 mg/dL ($P < 0.001$, $n = 10$) in diabetic rats at 12 weeks. Diabetic rats showed increase in food intake (26 ± 3 g/day) compared to the controls (16 ± 4 g/day). Despite increased food intake, the body weights of diabetic animals decreased significantly (178 ± 2.87 g, $P < 0.001$, $n = 10$) when compared to control animals (334.1 ± 8.07 g). The weight reduction in diabetic animals might be due to ketosis. Further, HbA1c levels were significantly higher (10.7 ± 0.2%, $P < 0.001$, $n = 10$) in diabetic rats compared to the controls (6.1 ± 0.14%).

Increased Expression of sHsps in Diabetic Retina. To determine the response of all sHsps during the chronic hyperglycemia, we analyzed the expression pattern of all sHsps and HSFs in retina by qRT-PCR and immunoblotting. However, of 10 sHsps, only Hsp27, αAC, αBC, Hsp20, and Hsp22 were detected in the retina. Expression of Hsp27 mRNA was significantly (18-fold) upregulated in diabetic rats (Fig. 1A), while, in contrast, its protein levels were downregulated (Figs. 2A, 2B). Interestingly, expression of αAC mRNA was remarkably upregulated (376-fold) in the retina of diabetic rats in comparison with controls (Fig. 1A). Correlating with mRNA, the protein levels of αAC also were increased significantly. Immunoblot analysis of anti-αAC antibody revealed two major bands in diabetic animals, in which the upper band represented the αA-insert and the lower band was αAC (Figs. 2A, 2B). Expression of αBC also was upregulated significantly at the mRNA (9.5-fold, Fig. 1A) and protein (Figs. 2A, 2B) levels. Although, expression levels of αAC and αBC were higher in the diabetic retina, relatively very low levels were detected in controls. Expression of Hsp20 was significantly downregulated at the mRNA (Fig. 1A) and protein (Figs. 2A, 2B) levels, whereas Hsp22 was significantly upregulated at the mRNA (Fig. 1A) and protein (Figs. 2A, 2B) levels in diabetic rats compared to controls.

Altered Expression of HSFs in the Diabetic Retina. To examine the regulation of sHsps, we analyzed the expression of three HSFs as well as HIF-1α in the retina under chronic

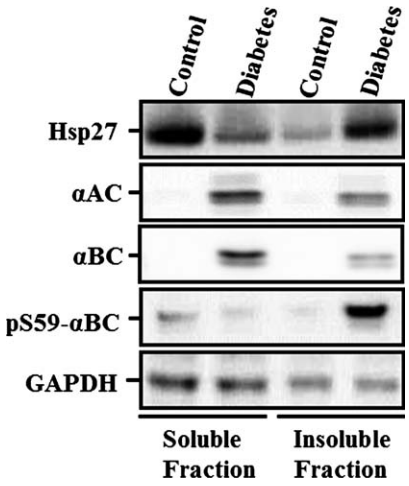

FIGURE 3. Solubility of sHsps in control and diabetic retinas. Diabetes reduced the solubility of Hsp27, αAC, αBC, and pS59-αBC in retinas as analyzed by Triton-X soluble assay. The retinal samples were fractionated into soluble and insoluble fractions, and subjected to immunoblotting.

hyperglycemic conditions. Surprisingly, the expression of HSF1 mRNA was significantly downregulated (Fig. 1B); consistent with transcript, the protein levels of HSF1 also were downregulated in diabetic rats (Figs. 2C, 2D). Although, no significant alterations were detected in HSF2 and HSF4 levels in the retina of diabetic rats (Figs. 1B, 2C, 2D), significant upregulation of HIF-1α at the mRNA (Fig. 1B) and protein (Figs. 2C, 2D) levels was detected in diabetic rats in comparison with controls.

Diabetes Decreases the Solubility of sHsps. To determine the soluble properties of sHsps under chronic hyperglycemic conditions, we analyzed the solubility of major sHsps Hsp27, αAC, αBC, and pS59-αBC by detergent solubility assay. All the four proteins were detected in Triton-X insoluble fraction, as their levels were translocated significantly from Triton-X soluble fraction to insoluble fraction in the retina of diabetic rats in comparison with age-matched controls (Fig. 3).

Kinase Mediated Phosphoregulation of αBC in Diabetes. Phosphorylation at S59 of αBC was decreased in the soluble fraction of diabetic retina with a concomitant increase in the insoluble fraction compared to controls (Fig. 3). Phosphorylation at S45, S19 of αBC was increased in the diabetic retina in comparison with controls (Figs. 4A, 4B). Furthermore, the S59 of αBC was phosphorylated by upstream p38MAPK. Therefore, we investigated the activation of p38MAPK by performing immunoblotting of total p38MAPK and p-p38MAPK in the retina of diabetic rats. Although there was no significant change in total p38MAPK, the p-p38MAPK levels were significantly increased in the retina of diabetic rats in comparison with controls, supporting the increased phosphorylation at S59 in diabetes (Figs. 4C, 4D).

Cellular Localization of sHsps and Phosphorylated αBCs in the Diabetic Retina. To provide support for the data on altered levels of sHsps and their phosphorylated forms in terms of their cellular localization, indirect immunofluorescence was performed on retinal sections for Hsp27, αAC, αBC, and pS59, pS45, pS19-αBC in control and diabetic rats.

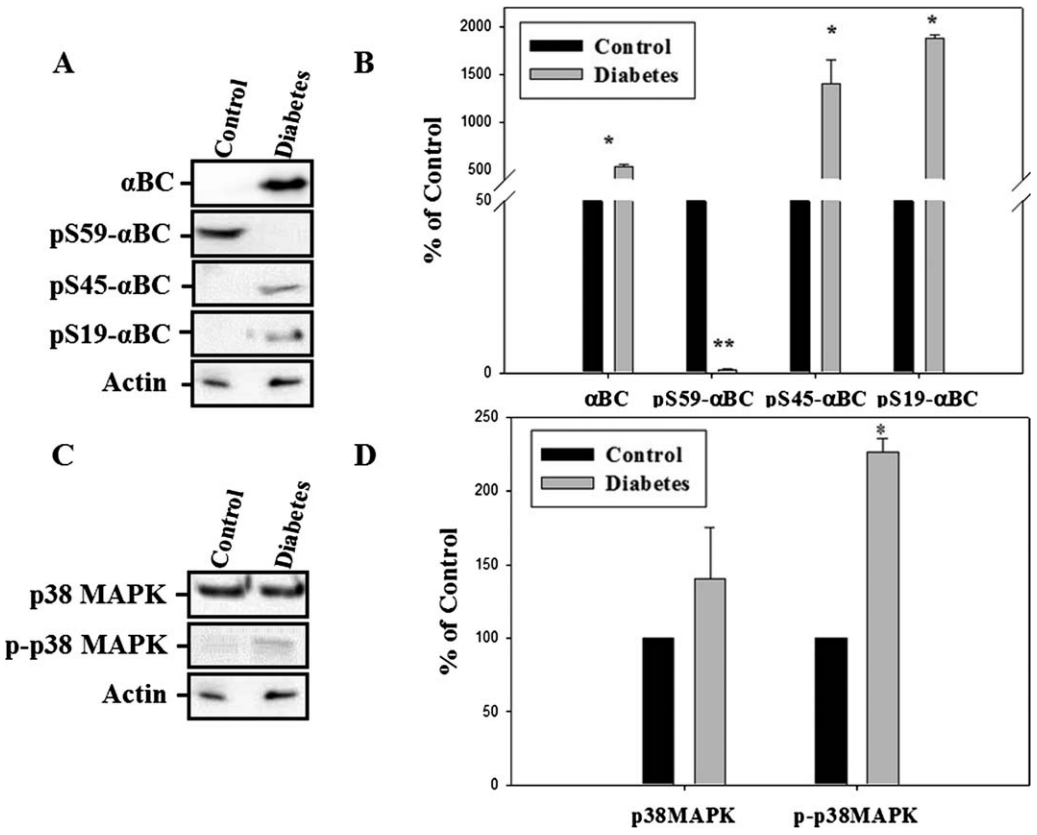

FIGURE 4. Immunoblot analysis of phosphorylated αBC (**A**) and p38MAPK (**C**) in retinas of control and diabetic rats. A total of 50 μg protein was loaded on SDS-PAGE for αBC, pS59, pS45, pS19-αBC, p38MAPK, and p-p38MAPK. Quantification of pS59, pS45, pS19-αBC (**B**) and p38MAPK, p-p38MAPK (**D**) immunoblots in retinas of control and diabetic rats; expression was normalized for actin expression and results are represented as percent of control. Data represent mean ± SEM of three independent experiments. $^{*}P < 0.05$, $^{**}P < 0.01$ compared to the control.

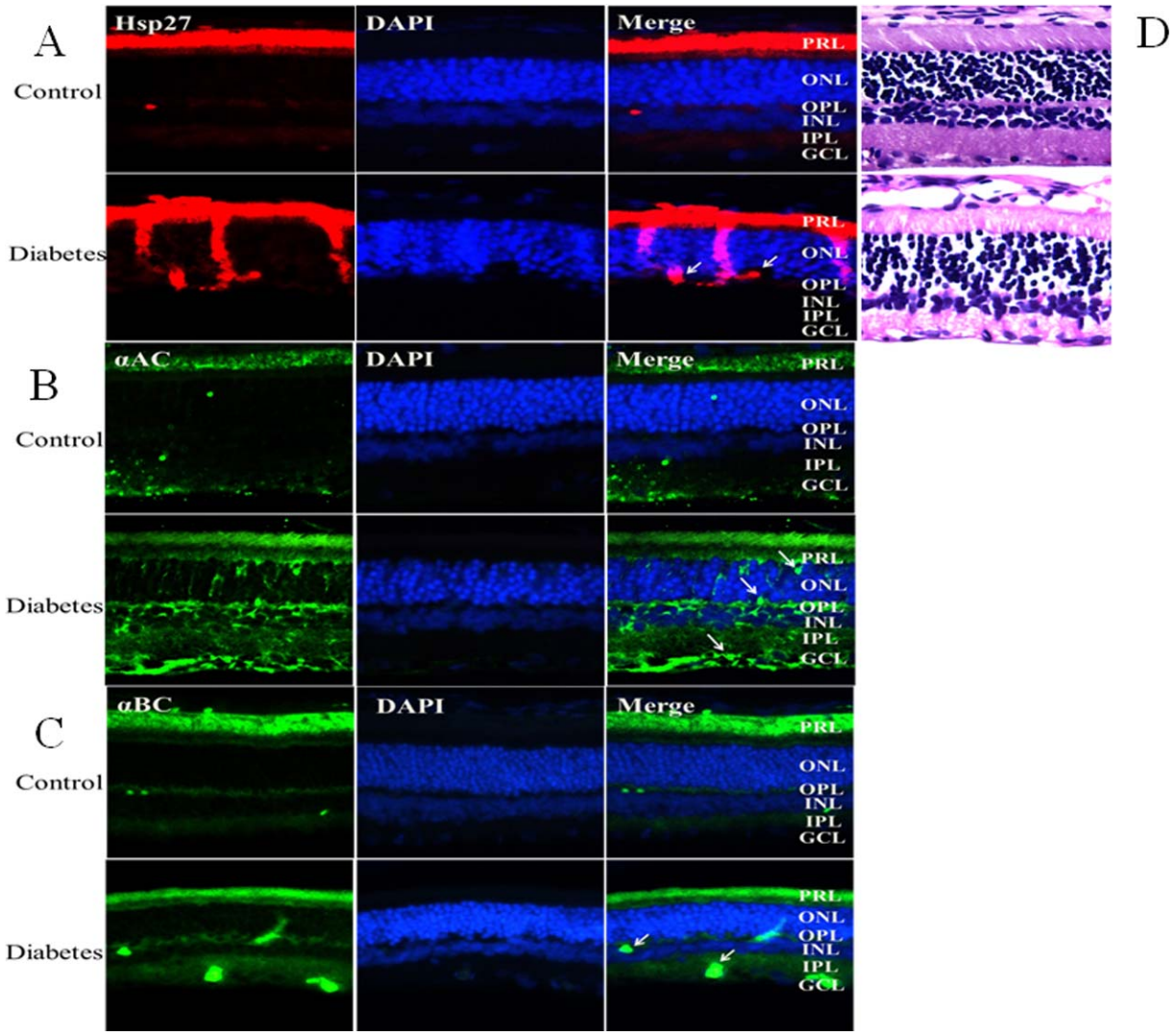

FIGURE 5. Cellular localization of sHsps in retina of control and diabetic rats. (**A**) Immunostaining of Hsp27 in retinas of control and diabetic rats. (**B**) Immunostaining of αAC in retinas of control and diabetic rats. (**C**) Immunostaining of αBC in retinas of control and diabetic rats. (**D**) Representative histology of control and diabetic rat retinas. Positive signals of Hsp27, αAC, and αBC in diabetic retinas are shown with *arrows*.

Immunostaining with Hsp27 antibody showed signal in the photoreceptor (PRL) and outer plexiform (OPL) layers in the control retina, while increased signal was seen in the PRL, outer nucleus layer (ONL), and OPL of diabetic rats (Fig. 5A). Immunostaining of αAC was confined to the PRL, inner plexiform layer (IPL), and ganglion cell layer (GCL) in control rats, but intense staining was distributed in all retinal layers of diabetic rats (Fig. 5B). Positive immunoreactivity of αBC was observed predominantly in the PRL, GCL, and, to a lesser degree, in the OPL, with increased staining (Fig. 5C) in diabetic rats compared to those of controls. Although there was a weak signal for pS59, pS45, and pS19-αBC in retina of control rats, intense staining was observed in diabetic rats. The increased immunostaining of pS59-αBC was localized in the PRL, OPL, and GCL in diabetic rats (Fig. 6A). While pS45-αBC was localized in the PRL, OPL, IPL, and GCL of control retinas, increased staining was observed in all retinal layers of diabetic rats (Fig. 6B). The pS19-αBC localized exclusively in the ONL of control retina, but strong immunostaining was detected in the PRL, OPL, INL, IPL, and GCL of diabetic rats (Fig. 6C). Further, hematoxylin and eosin (H&E)–stained images of control and diabetic retinas also presented to identify the various retinal layers represented in these figures (Figs. 5D, 6D).

DISCUSSION

In this study, we demonstrated the response of sHsps in the retina of a STZ-induced diabetic rat model. The major findings reported here are that of 10 sHsp family members, expression of Hsp27, αAC, αBC, Hsp20, and Hsp22 was seen in the retina. Of these, αAC, αBC, and Hsp22 were upregulated in the diabetic retina, while expression of Hsp20 was downregulated. Whereas Hsp27 mRNA levels were increased, while protein levels decreased, the expression of HSFs was either decreased or unaltered in the diabetic retina, and HIF-1α in conjunction with sHsps was upregulated in the diabetic retina. To our knowledge, this also is the first report in the diabetic retina of increased expression of pS59, pS45, and pS19-αBC; of demonstrated localization of sHsps and phosphorylated αBCs; and of reported extensive aggregation of Hsp27, pS59-αBC along with αAC and αBC. Previously, we reported the upregulation of α-crystallins in the diabetic rat retina.[16] Subsequently, many studies investigated the expression and

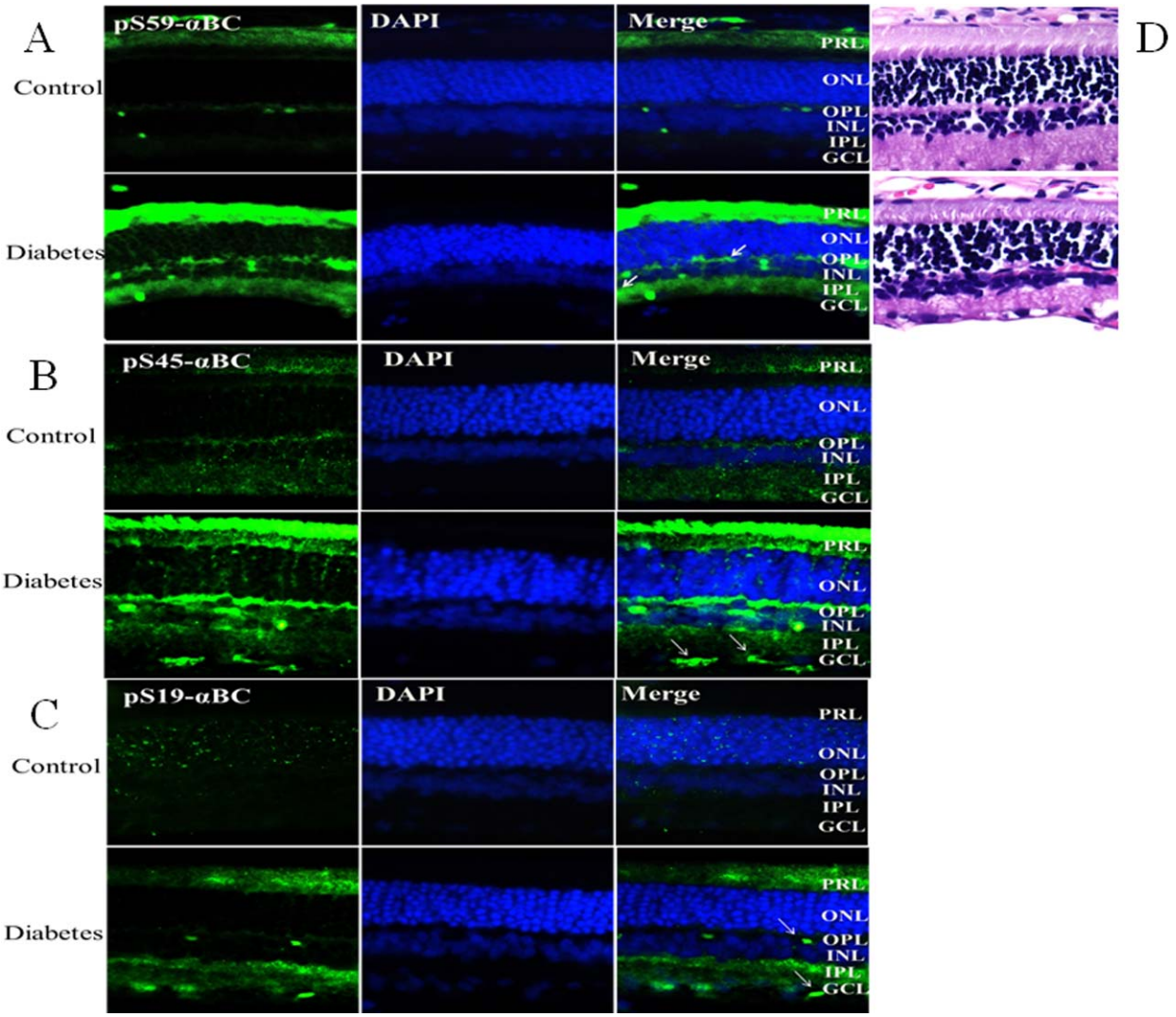

FIGURE 6. Cellular localization of phosphorylated αBCs in retinas of control and diabetic rats. (**A**) Immunostaining of pS59-αBC in retinas of control and diabetic rats. (**B**) Immunostaining of pS45-αBC in retinas of control and diabetic rats. (**C**) Immunostaining of pS19-αBC in retinas of control and diabetic rats. (**D**) Representative histology of control and diabetic rat retinas. Positive signals of pS59-αBC, pS45-αBC and pS19-αBC in diabetic retinas are shown with *arrows*.

role of α-crystallins in other rodent models of diabetes,[17,18,25] as well as in human DR patients.[26,27] Our study demonstrated the expression pattern of all detectable sHsps, HSFs, and phosphorylated αBCs in the retina of a diabetic rat model. The sHsps that could not be detected by qPCR and immunoblotting in the retina, MKBP, HSPB3, HSPB7, HSPB9, and HSPB10, are reported to be tissue-specific and expressed in those tissues, such as muscle, heart, and testis.[28,29]

The data obtained from transcript levels and protein expression analysis for sHsps were largely concurrent. The only discrepancy between transcript and protein was that of Hsp27 (Figs. 1A, 2A, 2B). Previous studies also reported similar observations that Hsp27 expression was elevated at the mRNA level, but decreased at the protein level under ischemic and stunned conditions in the heart,[30,31] and this might be due to reduction in transcriptional and translational rates. Further, increased immunostaining could be due to formation of smaller oligomers of Hsp27, thereby providing increased number of available epitopes for the antibody to bind. In support of this possibility, a study reported decrease in size of Hsp27 molecular aggregates, from large to small homo-oligomers in the diabetic kidney.[32] The increased expression of αAC and αBC at the mRNA and protein levels was consistent with the previous studies.[16,18,25] Furthermore, the very intense localization of αAC in the GCL layer of the diabetic retina indicated a role in protection of retinal neurons. Increased immunostaining of αBC in the PRL, OPL, IPL, and GCL of the diabetic rat retina also indicated that it might be protecting the different retinal cells from hyperglycemia-induced oxidative stress. To our knowledge, we reported for the first time the altered expression of Hsp20 and Hsp22 in the retina of diabetic rats (Figs. 1A, 2A, 2B). Very limited information is available about Hsp20 and Hsp22 in ocular tissues. The exact reason for downregulation of Hsp20 in the diabetic rat retina is unknown, but previous studies reported the downregulation of Hsp20 under ischemic conditions in neuroblastoma cells. Contrary, overexpression of Hsp20 protected neuroblastoma cells from ischemia/reperfusion injury by inhibiting apoptosis.[33] The Hsp22 prevents and/or helps in clearing the aggregated proteins,[34] and participates in regulation of proteolysis of unfolded proteins.[35] Therefore, increased expression of Hsp22 in the retina might be indicative of the unfolded protein response (UPR) and certain levels of neurotoxicity in STZ-induced experimental diabetic rats.

Despite the fact that sHsps expression is governed largely by HSFs, in our study, expression of HSF1, HSF2, and HSF4 either was unaltered or reduced in retina under diabetic conditions (Figs. 2B–D). Possible reason for decreased HSF1 expression could be explained by a couple of factors. The MAPKAP kinase 2 that gets activated during diabetes has been shown to be a potent inhibitor of HSF1.[36] Alternatively, glycogen synthase kinase-3 (GSK3) that gets elevated in diabetic patients[37] also has been shown to suppress HSF1 activation.[38] The reduction in expression of HSF1 during diabetes indicates that increased sHsps expression in diabetes might not be exerted through classical transcription factor HSF1. Indeed, elevated expression of the majority of sHsps in retina might be regulated in an HIF-1α–dependent manner in diabetic rats (Figs. 1B, 2C, 2D) as local hypoxia has been shown to stimulate HIF-1α in retina under hyperglycemic conditions.[39] Furthermore, some of the sHsps were not heat inducible, including αAC and Hsp20, and some are devoid of heat shock element (HSE) binding sequence, like αAC.[40] Nevertheless, tissue-specific and protein-specific transcription factors, including C-Maf, Pax, STAT, and BRN3, in regulating the induction of sHsps in various stress conditions and pathologies in various tissues cannot be ignored.[40]

In our study, we demonstrated that solubility of sHsps, including Hsp27, αAC, αBC, and pS59-αBC, was compromised under hyperglycemic conditions and accumulated as detergent-insoluble fraction in retina. It is possible that soluble complex of sHsp can transform to insoluble form when loaded with excessive nonnative substrate proteins, particularly when the other complimentary systems of protein quality control are unable to refold the aggregated or partially denatured proteins. This indicated that sHsps are overloaded with unfolded substrate proteins under uncontrolled hyperglycemic conditions and leading to insoluble aggregates.

The phosphorylation status of sHsps represents an important factor in determination of chaperone and antiapoptotic function in addition to their cellular distribution. Most sHsps have multiple phosphorylable serine residues. However, in our study, we focused mainly on the phosphorylation of major sHsp, αBC by immunoblotting. The pS59-αBC level was decreased in soluble fraction, whereas it was increased in insoluble fraction as well as in retinal sections of diabetic rats. The pS59-αBC is associated with increased and sustained chaperone activity,[41] and also is necessary for antiapoptotic activity.[42,43] The 35-week Otsuka Long–Evans Tokushima fatty (OLETF) rats of type-2 diabetes showed increased levels of pS59-αBC in retina.[44] Moreover, some previous reports demonstrated the decreased pS59-αBC in soluble fraction with concomitant increase in insoluble fraction in long-term heat-stressed H9C2 cells.[45] Hence, it is possible that 12 weeks of chronic hyperglycemia might reduce the solubility of pS59-αBC. The increased pS45-αBC levels in retina of 35-week OLETF rats with type 2 diabetes had a role in apoptosis,[44] and pseudophosphorylation of αBC at S45 showed protection of astrocytes against oxidative stress.[14] Furthermore, strong immunostaining of pS45-αBC in the diabetic retina indicated its role in hyperglycemia-induced cell death. Surprisingly, pS19-αBC also was increased in the diabetic retina, but the role of pS19-αBC is unknown so far. Although, the phosphorylation at S19 of αBC does not affect the protection status, the strong immunostaining in the PRL, OPL, IPL, and GCL in diabetic rats, and exclusively ONL in controls demonstrated a quite different role when compared to pS59 and pS45-αBC in retina. The p38MAPK/MAPK activated protein-2 signaling cascade can phosphorylate the S59 of αBC.[46] Herein, we show that diabetes increased the p38MAPK phosphorylation in retina. This finding is in agreement with previous reports of diabetes-induced activation of MAPK in retina.[47]

In summary, herein we reported the effect of experimental diabetes on expression of sHsps in retina in a comprehensive manner. However, the lack of general agreement on diabetes-induced changes in sHsps expression probably is due to differential response of transcriptional factors that regulate sHsps expression. Although further studies are required to clarify the role of sHsps in DR, taken together, these results suggested that the sHsp family is crucial for neuronal protection in DR and may aid in developing therapeutic strategies for DR.

Acknowledgments

The authors thank Sneha Jakotia for help in editing the manuscript.

Supported by grants from the Department of Science and Technology, and Department of Biotechnology, Government of India (GBR), and by a research fellowship from the University Grants Commission, Government of India (VSR).

Disclosure: **V.S. Reddy**, None; **G. Raghu**, None; **S.S. Reddy**, None; **A.K. Pasupulati**, None; **P. Suryanarayana**, None; **G.B. Reddy**, None

References

1. Resnikoff S, Pascolini D, Etya'ale D, et al. Global data on visual impairment in the year 2002. *Bull World Health Organ*. 2004; 82:844–851.
2. International Diabetes Federation. *The Diabetes Atlas,* 5th ed. 2011.
3. Muchova J, Liptakova A, Orszaghova Z, et al. Antioxidant systems in polymorphonuclear leucocytes of type 2 diabetes mellitus. *Diabet Med*. 1999;16:74–78.
4. Kumar A, Kaundal RK, Iyer S, Sharma SS. Effects of resveratrol on nerve functions, oxidative stress and DNA fragmentation in experimental diabetic neuropathy. *Life Sci*. 2007;80:1236–1244.
5. Giacco F, Brownlee M. Oxidative stress and diabetic complications. *Circ Res*. 107:1058–1070.
6. Kappe G, Franck E, Verschuure P, Boelens WC, Leunissen JA, de Jong WW. The human genome encodes 10 alpha-crystallin-related small heat shock proteins: HspB1-10. *Cell Stress Chaperones*. 2003;8:53–61.
7. Arrigo AP. [Heat shock proteins as molecular chaperones]. *Med Sci (Paris)*. 2005;21:619–625.
8. Sun Y, MacRae TH. Small heat shock proteins: molecular structure and chaperone function. *Cell Mol Life Sci*. 2005;62: 2460–2476.
9. Pirkkala L, Nykanen P, Sistonen L. Roles of the heat shock transcription factors in regulation of the heat shock response and beyond. *FASEB J*. 2001;15:1118–1131.
10. Whitlock NA, Agarwal N, Ma JX, Crosson CE. Hsp27 upregulation by HIF-1 signaling offers protection against retinal ischemia in rats. *Invest Ophthalmol Vis Sci*. 2005;46: 1092–1098.
11. David JC, Boelens WC, Grongnet JF. Up-regulation of heat shock protein HSP 20 in the hippocampus as an early response to hypoxia of the newborn. *J Neurochem*. 2006; 99:570–581.
12. Ecroyd H, Meehan S, Horwitz J, et al. Mimicking phosphorylation of alphaB-crystallin affects its chaperone activity. *Biochem J*. 2007;401:129–141.
13. Koteiche HA, McHaourab HS. Mechanism of chaperone function in small heat-shock proteins. Phosphorylation-induced activation of two-mode binding in alphaB-crystallin. *J Biol Chem*. 2003;278:10361–10367.
14. Li R, Reiser G. Phosphorylation of Ser45 and Ser59 of alphaB-crystallin and p38/extracellular regulated kinase activity determine alphaB-crystallin-mediated protection of rat brain

astrocytes from C2-ceramide- and staurosporine-induced cell death. *J Neurochem*. 118:354–364.

15. Kato K, Ito H, Kamei K, Inaguma Y, Iwamoto I, Saga S. Phosphorylation of alphaB-crystallin in mitotic cells and identification of enzymatic activities responsible for phosphorylation. *J Biol Chem*. 1998;273:28346–28354.
16. Kumar PA, Haseeb A, Suryanarayana P, Ehtesham NZ, Reddy GB. Elevated expression of alphaA- and alphaB-crystallins in streptozotocin-induced diabetic rat. *Arch Biochem Biophys*. 2005;444:77–83.
17. Fort PE, Freeman WM, Losiewicz MK, Singh RS, Gardner TW. The retinal proteome in experimental diabetic retinopathy: up-regulation of crystallins and reversal by systemic and periocular insulin. *Mol Cell Proteomics*. 2009;8:767–779.
18. Losiewicz MK, Fort PE. Diabetes impairs the neuroprotective properties of retinal alpha-crystallins. *Invest Ophthalmol Vis Sci*. 2011;52:5034–5042.
19. Kumar MS, Kapoor M, Sinha S, Reddy GB. Insights into hydrophobicity and the chaperone-like function of alphaA- and alphaB-crystallins: an isothermal titration calorimetric study. *J Biol Chem*. 2005;280:21726–21730.
20. Antonetti DA, Barber AJ, Khin S, Lieth E, Tarbell JM, Gardner TW. Vascular permeability in experimental diabetes is associated with reduced endothelial occludin content: vascular endothelial growth factor decreases occludin in retinal endothelial cells. Penn State Retina Research Group. *Diabetes*. 1998;47:1953–1959.
21. Barber AJ, Antonetti DA, Gardner TW. Altered expression of retinal occludin and glial fibrillary acidic protein in experimental diabetes. The Penn State Retina Research Group. *Invest Ophthalmol Vis Sci*. 2000;41:3561–3568.
22. Reiter CE, Sandirasegarane L, Wolpert EB, et al. Characterization of insulin signaling in rat retina in vivo and ex vivo. *Am J Physiol Endocrinol Metab*. 2003;285:E763–E774.
23. Barber AJ, Lieth E, Khin SA, Antonetti DA, Buchanan AG, Gardner TW. Neural apoptosis in the retina during experimental and human diabetes. Early onset and effect of insulin. *J Clin Invest*. 1998;102:783–791.
24. Zeng XX, Ng YK, Ling EA. Neuronal and microglial response in the retina of streptozotocin-induced diabetic rats. *Vis Neurosci*. 2000;17:463–471.
25. Kandpal RP, Rajasimha HK, Brooks MJ, et al. Transcriptome analysis using next generation sequencing reveals molecular signatures of diabetic retinopathy and efficacy of candidate drugs. *Mol Vis*. 18:1123–1146.
26. Dong Z, Kase S, Ando R, et al. Alphab-crystallin expression in epiretinal membrane of human proliferative diabetic retinopathy. *Retina*. 2012;32:1190–1196.
27. Kase S, Ishida S, Rao NA. Increased expression of alphaA-crystallin in human diabetic eye. *Int J Mol Med*. 28:505–511.
28. Garrido C, Paul C, Seigneuric R, Kampinga HH. The small heat shock proteins family: the long forgotten chaperones. *Int J Biochem Cell Biol*. 44:1588–1592.
29. Mymrikov EV, Seit-Nebi AS, Gusev NB. Large potentials of small heat shock proteins. *Physiol Rev*. 91:1123–1159.
30. Andres J, Sharma HS, Knoll R, et al. Expression of heat shock proteins in the normal and stunned porcine myocardium. *Cardiovasc Res*. 1993;27:1421–1429.
31. Simkhovich BZ, Marjoram P, Poizat C, Kedes L, Kloner RA. Brief episode of ischemia activates protective genetic program in rat heart: a gene chip study. *Cardiovasc Res*. 2003;59:450–459.
32. Dunlop ME, Muggli EE. Small heat shock protein alteration provides a mechanism to reduce mesangial cell contractility in diabetes and oxidative stress. *Kidney Int*. 2000;57:464–475.
33. Zeng L, Tan J, Hu Z, Lu W, Yang B. Hsp20 protects neuroblastoma cells from ischemia/reperfusion injury by inhibition of apoptosis via a mechanism that involves the mitochondrial pathways. *Curr Neurovasc Res*. 2010;7:281–287.
34. Seidel K, Vinet J, Dunnen WF, et al. The HSPB8-BAG3 chaperone complex is upregulated in astrocytes in the human brain affected by protein aggregation diseases. *Neuropathol Appl Neurobiol*. 2012;38:39–53.
35. Carra S, Seguin SJ, Lambert H, Landry J. HspB8 chaperone activity toward poly(Q)-containing proteins depends on its association with Bag3, a stimulator of macroautophagy. *J Biol Chem*. 2008;283:1437–1444.
36. Wang X, Khaleque MA, Zhao MJ, Zhong R, Gaestel M, Calderwood SK. Phosphorylation of HSF1 by MAPK-activated protein kinase 2 on serine 121, inhibits transcriptional activity and promotes HSP90 binding. *J Biol Chem*. 2006;281:782–791.
37. Nikoulina SE, Ciaraldi TP, Mudaliar S, Mohideen P, Carter L, Henry RR. Potential role of glycogen synthase kinase-3 in skeletal muscle insulin resistance of type 2 diabetes. *Diabetes*. 2000;49:263–271.
38. He B, Meng YH, Mivechi NF. Glycogen synthase kinase 3beta and extracellular signal-regulated kinase inactivate heat shock transcription factor 1 by facilitating the disappearance of transcriptionally active granules after heat shock. *Mol Cell Biol*. 1998;18:6624–6633.
39. Ly A, Yee P, Vessey KA, Phipps JA, Jobling AI, Fletcher EL. Early inner retinal astrocyte dysfunction during diabetes and development of hypoxia, retinal stress, and neuronal functional loss. *Invest Ophthalmol Vis Sci*. 2011;52:9316–9326.
40. de Thonel A, Le Mouel A, Mezger V. Transcriptional regulation of small HSP-HSF1 and beyond. *Int J Biol Cell Biol*. 2012;44:1593–1612.
41. Kase S, He S, Sonoda S, et al. AlphaB-crystallin regulation of angiogenesis by modulation of VEGF. *Blood*. 115:3398–3406.
42. Hoover HE, Thuerauf DJ, Martindale JJ, Glembotski CC. Alpha B-crystallin gene induction and phosphorylation by MKK6-activated p38. A potential role for alpha B-crystallin as a target of the p38 branch of the cardiac stress response. *J Biol Chem*. 2000;275:23825–23833.
43. Morrison LE, Hoover HE, Thuerauf DJ, Glembotski CC. Mimicking phosphorylation of alphaB-crystallin on serine-59 is necessary and sufficient to provide maximal protection of cardiac myocytes from apoptosis. *Circ Res*. 2003;92:203–211.
44. Kim YH, Choi MY, Kim YS, et al. Protein kinase C delta regulates anti-apoptotic alphaB-crystallin in the retina of type 2 diabetes. *Neurobiol Dis*. 2007;28:293–303.
45. Singh BN, Rao KS, Ramakrishna T, Rangaraj N, Rao ChM. Association of alphaB-crystallin, a small heat shock protein, with actin: role in modulating actin filament dynamics in vivo. *J Mol Biol*. 2007;366:756–767.
46. Ito H, Okamoto K, Nakayama H, Isobe T, Kato K. Phosphorylation of alphaB-crystallin in response to various types of stress. *J Biol Chem*. 1997;272:29934–29941.
47. Du Y, Tang J, Li G, et al. Effects of p38 MAPK inhibition on early stages of diabetic retinopathy and sensory nerve function. *Invest Ophthalmol Vis Sci*. 51:2158–2164.

Investigative Ophthalmology & Visual Science